Journal of Alloys and Compounds 509 (2011) 8144–8148

Contents lists available at ScienceDirect

Journal of Alloys and Compounds

journal homepage: www.elsevier.com/locate/jallcom

Coexistence of room temperature ferroelectricity and ferrimagnetism in multiferroic $BiFeO_3$–$Bi_{0.5}Na_{0.5}TiO_3$ solid solution

Z.M. Tian, C.H. Wang, S.L. Yuan*, M.S. Wu, Z.Z. Ma, H.N. Duan, L. Chen

School of Physics, Huazhong University of Science and Technology, Wuhan 430074, PR China

ARTICLE INFO

Article history:
Received 15 November 2010
Received in revised form 22 May 2011
Accepted 23 May 2011
Available online 30 May 2011

Keywords:
Ferroelectricity
Ferrimagnetism
$BiFeO_3$

ABSTRACT

The structure, ferroelectric and magnetic properties of $(1-x)BiFeO_3$–$xBi_{0.5}Na_{0.5}TiO_3$ ($x = 0.37$) solid solution fabricated by a sol–gel method have been investigated. X-ray diffraction and Raman spectroscopy measurements show a single-phase perovskite structure with no impurities identified. Compared with pure $BiFeO_3$, the coexistence of ferroelectricity and ferrimagnetism have been observed at room temperature for the solution with remnant polarization $P_r = 1.41\ \mu C/cm^2$ and remnant magnetization $M_r = 0.054$ emu/g. Importantly, a magnetic transition from ferrimagnetic (FM) ordering to paramagnetic (PM) state is observed, with Curie temperature $T_C \sim 330$ K, being explained in terms of the suppression of cycloid spin configuration by the structural distortion.

1. Introduction

The single-phase multiferroics which exhibit simultaneous ferroelectricity and magnetism, have attracted increasing interest because of their potential applications in multifunctional devices as well as their fascinating fundamental physics [1,2]. Among all known multiferroics, $BiFeO_3$ (BF) is one of the most promising materials for technological applications, being characterized by high ferroelectric (FE) Curie temperature ($T_{CE} \sim 1103$ K) and antiferromagnetic (AFM) Néel temperature ($T_N \sim 643$ K) [3,4]. This compound crystallizes in the rhombohedral distorted perovskite structure with space group *R3c* at room temperature [5]. Besides, it exhibits canted G-type AFM order combined with space-modulated spin structure on a long wavelength of 620 Å, which prevents the observation of weak ferromagnetism driven by Dzyaloshinskii–Moriya (D–M) interactions [6,7], hence inhibits the observation of linear magnetoelectric effect [8]. With respect to bulk BF compounds, the relatively high electrical conductivity and unwanted secondary phases make it difficult to obtain a well saturated electrical polarization. To overcome these deficiencies, efforts are made to introduce perovskite compounds, such as $BaTiO_3$, $PbTiO_3$, $Bi_4Ti_3O_{12}$ and $Ba(Fe_{0.5}Nb_{0.5})O_3$ into BF to form solid solutions [9–12]. In these crystalline solutions, the formation of secondary phases is suppressed and the perovskite structure is stable. It has been proved to be a very effective method in improving the ferroelectric (FE) properties and enhancing the formation of crystalline solutions. In contrast, no evidence of magnetic transition from ferro/ferrimagnetic (FM) ordering to paramagnetic (PM) state above room temperature was reported.

In this work, $(Bi_{0.5}Na_{0.5})TiO_3$ (BNT) is chosen to form a solid solution with BF, because it is one of lead-free perovskite ferroelectric materials with FE Curie temperature $T_{CE} \sim 593$ K and possesses rhombohedral symmetry with space group *R3c* similar to that of BF [13,14]. The structure, ferroelectric and magnetic properties of $(1-x)BiFeO_3$–$x(Bi_{0.5}Na_{0.5})TiO_3$ ($x = 0.37$) solid solution which presents a remarkable coexistence of ferroelectricity and ferrimagnetism above room temperature have been investigated.

2. Experimental details

The $(1-x)BiFeO_3$–$xBi_{0.5}Na_{0.5}TiO_3$ ($x = 0.37$) (BF–BNT) solid solution was fabricated by a sol–gel method as described in Ref. [15]. Analytical-grade $Bi(NO_3)_3{\cdot}5H_2O$, $Fe(NO_3)_3{\cdot}9H_2O$, $NaNO_3$ and $Ti[OCH(CH_3)_2]_4$ were chosen as raw starting materials, with citric acid and distilled water as solvents. Firstly, appropriate $Bi(NO_3)_3{\cdot}5H_2O$, $Fe(NO_3)_3{\cdot}9H_2O$, $NaNO_3$ and $Ti[OCH(CH_3)_2]_4$ were dissolved into a solution of citric acid to form the BF–BNT precursor solution. Subsequently, the solutions were adjusted to a pH value of 7–7.5 by adding ammonia and dried at 120 °C to form the dried gel. The dried gel was calcined at 500 °C for 5 h to form the precursor powders. Finally, the powders were pressed into pellets and sintered at 950 °C for 3 h.

The structure of the samples was characterized by X-ray diffraction (XRD) on a Philips Panalytical X'pert diffractometer with Cu Kα radiation. Raman spectroscopy was performed in a Raman spectrometer (Renishaw, RM-1000) employing an Ar+ laser for excitation ($\lambda = 514$ nm). X-ray photoelectron spectroscopy (XPS) (PHI Quantera SXM) was used to examine the state of Fe *2p* electrons. The ferroelectric properties and leakage currents were measured using a standard ferroelectric test system (Premier II, Radiant Technologies). The magnetic properties were investigated in a commercial physical property measurement system (PPMS, Quantum Design).

* Corresponding author.
E-mail address: yuansl@hust.edu.cn (S.L. Yuan).

0925-8388/$ – see front matter © 2011 Elsevier B.V. All rights reserved.
doi:10.1016/j.jallcom.2011.05.083

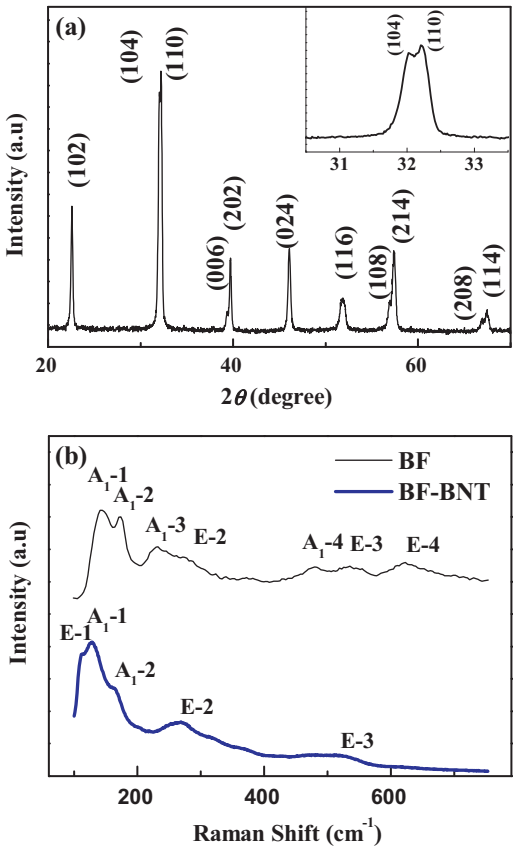

Fig. 1. (a) The XRD pattern for $(1-x)BiFeO_3$–$xBi_{0.5}Na_{0.5}TiO_3$ ($x = 0.37$) solid solution. The inset shows the magnified patterns of (1 0 4) and (1 1 0) peaks. (b) The Raman spectra for pure BF and BF–BNT solid solution.

3. Results and discussion

Fig. 1(a) shows the XRD pattern of BF–BNT ceramics, which indicates a single-phase perovskite structure with no trace of other impurity phases (e.g. Fe_2O_3, Bi_2O_3, TiO_2, etc.) within the uncertainty of XRD. The existence of splitting peaks around 31° and 39° suggests the distorted rhombohedral R3c structure, as shown in the inset of Fig. 1(a). The calculated lattice parameters are $a = b = 5.5515(1)$ Å and $c = 13.7340(2)$ Å, in contrast to the lattice $a = b = 5.5820(1)$ Å, $c = 13.8581(1)$ Å for the parent compound $BiFeO_3$. This slight contraction of the unit volume can be attributed to the difference of the ionic radius at the B-site of the perovskite, since the radius of Ti^{4+} ion (0.605 Å) is smaller than the one of Fe^{3+} ion (0.645 Å), while the A-site ions have similar atomic radius (Bi^{3+} = 1.38 Å, Na^{+} = 1.39 Å). The Raman spectra of pure BF and BF–BNT ceramics are shown in Fig. 1(b). Compared with pure BF, the disappearance of A_1-3 modes and the emergence of E-1 mode in BF–BNT solution reveals the incorporation of the Na and Ti ions into the BF lattice. Moreover, the A_1-1 modes are associated with Fe ions [16], their shift to lower frequencies indicating the compressive structural distortion for the solution, consistent with the XRD results.

The ferroelectric hysteresis loops for the BF–BNT solution were measured at room temperature at 10 Hz, as shown in Fig. 2. A typical ferroelectric hysteresis with remnant polarization $P_r = 1.41$ μC/cm^2 and coercive field $H_c = 33.7$ kV/cm is obtained. The measured P_r is comparable to that of $BiFeO_3$–$PbTiO_3$ solutions prepared by Singh et al. [17], but it is much lower than the theoretically predicted value [18]. This can be due to the high leakage current as shown in the inset of Fig. 2, where the leaky features can be related to the oxygen vacancies or valence fluctuation of the transition metal ions.

To evaluate the valence states of the Fe and Ti ions, X-ray photoelectron spectroscopy (XPS) for Bi 4*f* (b), Ti 2*p* (c), and Fe 2*p* (d) core level binding energy spectra of BF–BNT are presented in Fig. 3. Two most intense peaks at 158.9 and 164.2 eV are assigned to Bi^{3+} $4f_{7/2}$ and $4f_{5/2}$ states, as shown in Fig. 3(b). In Ti 2*p* XPS spectra, even if

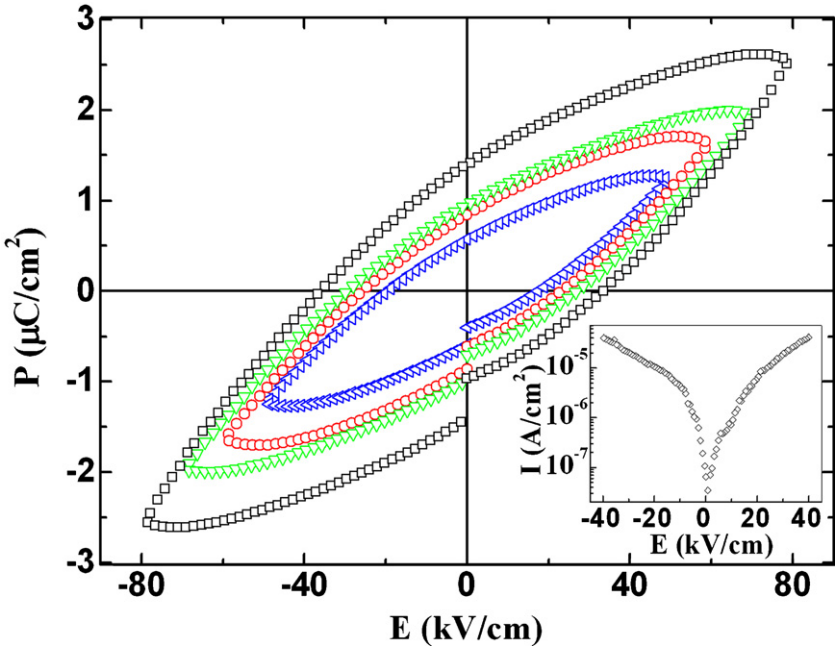

Fig. 2. Ferroelectric hysteresis loops (P–E) for the BF–BNT solid solution measured at room temperature. The inset shows the leakage current as a function of applied electric field.

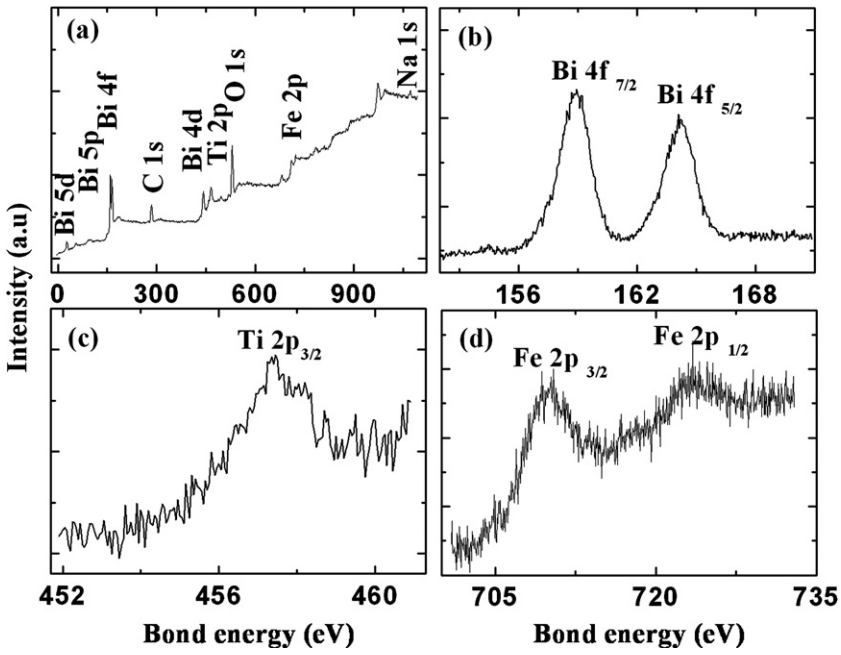

Fig. 3. The XPS spectrum of BF–BNT solution.

the noise to signal ratio is high, the binding energy of Ti $2p_{3/2}$ is near 458.0 eV indicating a valence +4 for Ti element, in accordance with the Ti $2p_{3/2}$ for Ti^{4+} compounds in Ref. [19]. Additionally, the core level binding energies of Fe $2p_{3/2}$ and Fe $2p_{1/2}$ are estimated to be about 710.1 and 723.3 eV, respectively. Considering that the peaks of Fe^{2+} $2p_{3/2}$ and Fe^{3+} $2p_{3/2}$ are appearing normally at 709.5 and 711.2 eV [20], our results indicate that the valence of Fe element is a mixture of Fe^{3+} and Fe^{2+} with Fe^{3+} prevailing. In order to keep the charge balance, the slight deficiency will possibly lead to oxygen deficiency, which is common for perovskite oxides. In this case, the variable oxidation states of Fe element combined with the oxygen vacancies can be responsible for the high leakage current.

Fig. 4 shows the magnetic hysteresis loops (M–H) measured at different temperatures. A linear magnetic field dependence of magnetization is observed at 350 K indicating a paramagnetic (PM) state. Contrastly, the room temperature FM characteristics are confirmed by the magnetic hysteresis loop shape, with remnant magnetization $M_r = 0.054$ emu/g and coercive field $H_c = 1.05$ kOe. This reveals that a magnetic transition takes place in the temperature range from 300 K to 350 K. To check this magnetic transition,

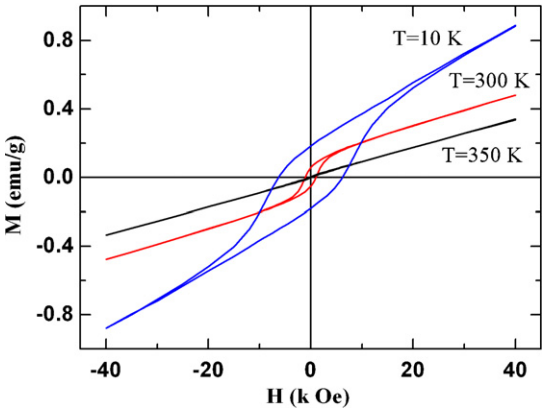

Fig. 4. Magnetic hysteresis loops for the BF–BNT solid solution measured at different temperatures.

the temperature dependence of zero-field cooled (ZFC) and field cooled (FC) magnetization curves was measured in the temperature range of 10–350 K at applied fields up to 40 kOe. As shown in Fig. 5(a), a magnetic transition from ferromagnetic (FM) ordering to paramagnetic (PM) state is observed at $T_c \sim 330$ K, where the ZFC curve shows a peak. Below this temperature, the ZFC and FC magnetization curves show a large discrepancy. Furthermore, this discrepancy shifts to lower temperatures and disappears with the increase of the magnetic field. This magnetic behavior is very interesting and basically different from that reported for A-site doped $BiFeO_3$ by a variety of ions (e.g. La, Sm, Eu, etc.) [21–23], or solutions with $BaTiO_3$ and $PbTiO_3$ [9,24], where no obvious FM–PM transition is observed.

To further clarify if the transition near 330 K is a ferrimagnetic order one rather than the spin reorientation and/or the spin-glassy transition as observed in single-crystal $BiFeO_3$ [25], the ac susceptibility versus different frequencies (f) from 97 to 9997 Hz has been measured. As seen from Fig. 6, both $\chi'(T)$ and $\chi''(T)$ show a clear peak at 330 K confirming the magnetic transition. The location of the peak is independent of the frequency, ruling out the possibility of the existence of the spin-glassy transition. Nevertheless, before ascribing the observed FM to be intrinsic, it is necessary to exclude the contribution from impurity phases such as γ-Fe_2O_3, $Bi_2Fe_4O_9$, $Bi_{25}FeO_{40}$. Firstly, the BF–BNT has a larger H_c (~1 kOe) than γ-Fe_2O_3 impurity (<100 Oe), which exclude the possible origination from γ-Fe_2O_3 impurity. Secondly, the impurities of $Bi_{25}Fe_2O_{39}$ and $Bi_{25}FeO_{40}$ in some of these samples are paramagnetic or only FM at low temperatures, and $Bi_2Fe_4O_9$ is antiferromagnetic with $T_N \sim 260$ K [15]. Based on above considerations, the ferrimagnetic ordering transition in this system can be considered as intrinsic and ascribed to the collapse of the cycloid spin structure by a structural distortion due to the Dzyaloshinskii–Moriya (D–M) interaction [6,7], releasing the latent magnetization locked within the cycloid spin structure. As for this solution, incorporating Na^+ cations on Bi^{3+} sites and Ti^{4+} on Fe^{3+} sites can lead to a random arrangement of Fe^{3+} and Ti^{4+} ions at the B sites. In this case, a superexchange in the disordered regions through Fe^{3+}–O–Fe^{3+} is expected, and this superexchange interaction is FM coupling [26,27], which can be responsible for the FM observed at room temperature. A similar

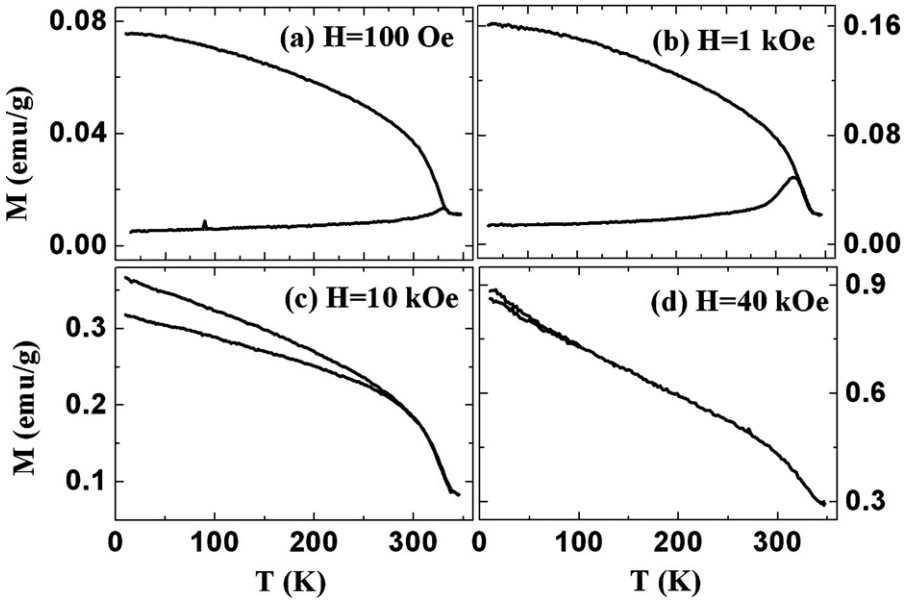

Fig. 5. ZFC and FC magnetization curves measured at different magnetic fields for BF–BNT solid solution.

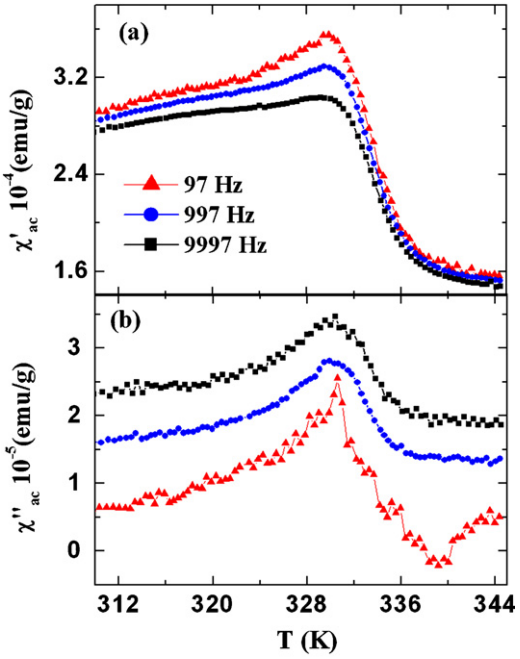

Fig. 6. The temperature dependence of the ac susceptibility versus frequency for BF-BNT solid solution. The real (χ') and imaginary (χ'') part of the susceptibility are shown in (a) and (b), respectively.

mechanism has also been reported by Wei et al. [28] in nonmagnetic Fe-site doped $BiFeO_3$, where the neighboring Fe^{3+} ions can be FM coupling via long-range superexchange of the Fe^{3+}–O–Ti–O–Fe^{3+} pathway.

4. Conclusions

In summary, single-phase $(1-x)BiFeO_3$–$xBi_{0.5}Na_{0.5}TiO_3$ ($x = 0.37$) multiferroic solid solutions have been synthesized by a sol–gel method, which is confirmed by the XRD and Raman spectroscopy measurements. This solution shows the coexistence of ferroelectricity and ferrimagnetism at room temperature with remnant polarization $P_r = 1.41\ \mu C/cm^2$ and remnant magnetization $M_r = 0.054$ emu/g, respectively. Furthermore, FM to PM transition is obtained with Curie temperature $T_C \sim 330$ K, which is ascribed to the suppression of cycloid spin configuration by the structural distortion.

Acknowledgments

This work was supported by the National Science Foundation of China (Grant No. 51002060), by the Foundation from the ministry of the National Education (Grant Nos. 309020 & 20090142120069), by the foundation Research funds for the central Universities (Grant Nos. HUST: 2010ZD006, 2010QN012). We would like to thank the staff of Analysis Center of HUST for their assistance in various measurements.

References

[1] N.A. Spaldin, M. Fiebig, Science 309 (2005) 391.
[2] R. Ramesh, N.A. Spaldin, Nat. Mater. 6 (2007) 21.
[3] N.A. Hill, J. Phys. Chem. B 104 (2000) 6694.
[4] C. Tabares-Munoz, J.P. Rivera, A. Monnier, H. Schmid, Jpn. J. Appl. Phys. Lett. Part 1 (24) (1985) 1051.
[5] A.J. Jacobson, B.E.F. Fender, J. Phys. C 8 (1975) 844.
[6] I.E. Dzialoshinskii, Sov. Phys. JETP 5 (1957) 1259.
[7] T. Moriya, Phys. Rev. 120 (1960) 91.
[8] F. Zavaliche, R.R. Das, D.M. Kim, C.B. Eom, S.Y. Yang, P. Shafer, R. Ramesh, Appl. Phys. Lett. 87 (2005) 182912.
[9] F.P. Gheorghiu, A. Ianculescu, P. Postolache, N. Lupu, M. Dobromir, D. Luca, L. Mitoseriu, J. Alloy Compd. 506 (2010) 862.
[10] S. Bhattacharjee, V. Pandey, R.K. Kotnala, D. Pandey, Appl. Phys. Lett. 94 (2009) 012906.
[11] X.W. Dong, K.F. Wang, J.G. Wan, J.S. Zhu, J.M. Liu, J. Appl. Phys. 103 (2008) 094101.
[12] H. Paik, H. Hwang, K. No, Appl. Phys. Lett. 90 (2007) 042908.
[13] T. Takenaka, K. Maruyama, K. Sakata, Jpn. J. Appl. Phys. Part 1 (30) (1991) 2236.
[14] G.A. Smolensky, V.A. Isupov, A.Y. Agranovskaya, N.N. Krainik, Sov. Phys. Solid State 2 (1961) 2651.
[15] Z.M. Tian, S.L. Yuan, X.L. Wang, X.F. Zheng, S.Y. Yin, C.H. Wang, L. Liu, J. Appl. Phys. 106 (2009) 103912.
[16] P. Kharel, S. Talebi, B. Ramachandran, A. Dixit, V.M. Naik, M.B. Sahana, C. Sudakar, R. Naik, M.S.R. Rao, G. Lawes, J. Phys.: Condens. Matter 21 (2009) 036001.
[17] K. Singh, R.K. Kotnala, M. Singh, Appl. Phys. Lett. 93 (2008) 212902.
[18] J.B. Neaton, C. Ederer, U.V. Waghmare, N.A. Spaldin, K.M. Rabe, Phys. Rev. B 71 (2005) 014113.

[19] V.V. Atuchin, V.G. Kesler, N.V. Pervukhina, Z.M. Zhang, J. Electron. Spectrosc. Relat. Phenom. 152 (2006) 18.
[20] T. Schedel-Niedrig, W. Weiss, R. Schlögl, Phys. Rev. B 52 (1995) 17449.
[21] K. Prashanthi, B.A. Chalke, K.C. Barick, A. Das, I. Dhiman, V.R. Palkar, Solid. Stat. Commun. 149 (2009) 188.
[22] D. Maurya, H. Thota, A. Garg, B. Pandey, P. Chand, H.C. Verma, J. Phys.: Condens. Matter 21 (2009) 026007.
[23] V.R. Reddy, D. Kothari, A. Gupta, S.M. Gupta, Appl. Phys. Lett. 94 (2009) 082505.
[24] W.M. Zhu, Z.G. Ye, Appl. Phys. Lett. 89 (2006) 232904.
[25] M.K. Singh, W. Prellier, M.P. Singh, R.S. Katiyar, J.F. Scott, Phys. Rev. B 77 (2008) 144403.
[26] A. Kumar, G.L. Sharma, R.S. Katiyar, J.F. Scott, R. Pirc, R. Blinc, J. Phys.: Condens. Matter 21 (2009) 382204.
[27] R.A.M. Gotardo, I.A. Santos, L.F. Cotica, E.R. Botero, D. Garcia, J.A. Eiras, Scripta Mater. 61 (2009) 508.
[28] J. Wei, R. Haumont, R. Jarrier, P. Berhtet, B. Dkhil, Appl. Phys. Lett. 96 (2010) 102509.